The Magellanic System: Stars, Gas, and Galaxies
Proceedings IAU Symposium No. 256, 2008
Jacco Th. van Loon & Joana M. Oliveira, eds.

doi:10.1017/S1743921308028196

Survey of the Magellanic Clouds at 4.8 and 8.64 GHz

John Dickel[1], Robert A. Gruendl[2], Vincent McIntyre[3], Shaun Amy[3] and Douglas Milne[3]

[1]Physics and Astronomy Bldng., MSC07-4220, U. New Mexico, Albuquerque NM 87131, USA
email: johnd@phys.unm.edu

[2]UI Astronomy Bldng, 1002 West Green St, Urbana IL 61801, USA
email: gruendl@astro.illinois.edu

[3]ATNF-CSIRO Box 76. Epping NSW 1710, Australia
email: Vincent.McIntyre@atnf.csiro.au, Shaun.Amy@atnf.csiro.au, D_K_Milne@hotmail.com

Abstract. Detailed 4.8 and 8.64 GHz radio images of the entire Large and Small Magellanic Clouds with half-power beamwidths of 35″ at 4.8 GHz and 22″ at 8.64 GHz have been obtained using the Australia Telescope Compact Array. Full polarimetric observations were made. Several thousand mosaic positions were used to cover an area of 6° on a side for the LMC and 4.5° for the SMC. These images have sufficient spatial resolution (∼8 and 5 pc, respectively) and sensitivity (3σ of 1.5 mJy beam^{-1}) to identify most of the individual supernova remnants and H II regions and also, in combination with available data from the Parkes 64-m telescope, the structure of the smooth emission in these galaxies. We have recently revised the early data analysis (Dickel *et al.* 2005) by increasing the CLEAN cutoff limit to recover more intermediate-spacing data and thus present more accurate brightnesses for extended sources. In addition, limited data using the sixth antenna at 4.5 − 6 km baselines are available to distinguish bright point sources (< 3″ and 2″, respectively) and to help estimate sizes of individual sources smaller than the resolution of the full survey. The resulting database will be valuable for statistical studies and comparisons with X-ray, optical, and infrared surveys of the LMC with similar resolution.

Keywords. instrumentation: interferometers, surveys, ISM: general, Magellanic Clouds

1. Introduction

Radio continuum observations of the Magellanic Clouds can be used to measure both thermal emission from H II regions, polarized synchrotron emission from supernova remnants (SNRs), and the distributed interstellar medium. The common distance of all the sources offers an important evaluation of their statistical properties. The thermal emission has a nearly flat radio spectrum whereas the synchrotron emission, from relativistic electrons accelerated in shocks and the magnetic fields of SNRs, has a power-law spectrum with brighter emission at lower frequencies to help distinguish the different objects.

Three important sources of stellar energy in the ISM are UV radiation, fast stellar winds, and supernovae. Thus the radio observations supply a vital component in studies of these energy sources by tracing the contributions from both the photoionized and shock-ionized material and (through polarimetry) showing the orientation of magnetic field lines, even deep within highly obscured regions like molecular clouds. In combination with optical line emission (Smith *et al.* 2005), X-ray images (Snowden 1999), and infrared images (Meixner 2008) from the new generation surveys at those wavelengths, high-resolution radio continuum imaging will help to construct a complete physical picture of stellar feedback in the Magellanic Clouds.

The survey can also probe background objects in both total intensity and polarimetry, to determine their properties and any significant effects caused by passage of their radiation through the Magellanic Clouds.

2. Equipment and Observations

The observations were made with the Australia Telescope Compact Array (*ATCA*) using two configurations of the five movable 22-m dishes to give 19 independent baselines with spacings from 30 out to 367 meters. Short spacings were recovered by adding data from the Parkes 64-m dish (Haynes *et al.* 1991). The normalization of the data sets from the two telescopes was done by using the flux density calibrations of the primary source PKS 1934–638 at each wavelength. The slight differences in frequency and a re-evaluation of the scale between the observations with the two instruments were less than 10% and were accounted for. Combination of all the data gave half-power beamwidths of 35″ at 4.8 GHz and 22″ at 8.64 GHz. Data were also available from a sixth antenna about 4.5 km from the other five to further evaluate the sizes of unresolved sources using an incomplete $2 - 3''$ interference pattern.

The final images are mosaics of 6336 overlapping pointings for the LMC and 3564 for the SMC. Each pointing was observed for 20 −24 seconds at each of eight approximately uniformly spaced hour angles for each of the two telescope configurations resulting in an integration time of > 320 sec per point and reasonable coverage of orientations and telescope spacings for the aperture synthesis.

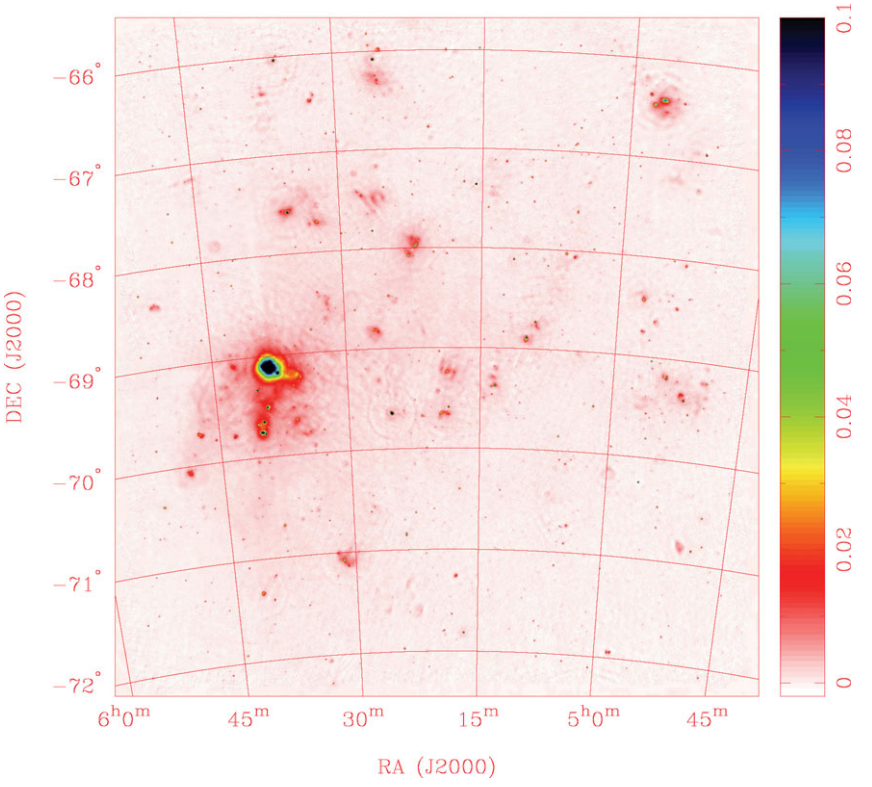

Figure 1. Total intensity image of the Large Magellanic Cloud at 4.8 GHz. The units of surface brightness in this and all subsequent images are Jy beam^{-1}.

https://doi.org/10.1017/S1743921308028196 Published online by Cambridge University Press

As part of the image restoration process, they have been CLEANed (Högbom 1973) down to a cutoff level of 2 mJy beam^{-1} which is about 5 times the theoretical noise level. Experimentation with deeper clean levels resulted in the loss of some of the faint smooth emission from the shorter spacings of the *ATCA* and thus loss of structure on the extended sources.

The instrumental polarization was evaluated by observing the brightest spot in the H II region 30 Doradus. There was some off-axis polarization as well as some toward the peak but the instrumental effects everywhere were less than 0.14% at 4.8 GHz and 1.25% at 8.64 GHz. Because almost all of the sources in the images had surface brightnesses fainter than about 100 mJy beam^{-1}, the polarization measurements were generally limited by the signal-to-noise ratio rather than instrumental effects. Particularly at 8.64 GHz, few sources have bright enough polarization for reliable measurement. The only polarimetric data available from Parkes are for the LMC at 4.8 GHz.

We note two features of the 8.64 GHz images. The first is that the smaller beamwidth at that frequency reduces the surface brightness per beam and thus the background noise is relatively higher. Second, atmospheric variations affect the higher frequency more so that the phase can drift more during an observation and smear a small diameter source over a larger area.

3. The Images

3.1. *LMC*

The full image of the LMC (Fig. 1) at 4.8 GHz is dominated by the 30-Dor complex (Bode 1801) and the ridge to the south of it which is very prominent in molecular line emission as first detected by Cohen *et al.* (1988). Although there are a number of H II regions and supernova remnants located along the region of the bar in the LMC, there are just as many scattered throughout the entire galaxy, particularly to the north. Thus, recent stellar birth and death does not seem to be exclusively associated with the bar.

To illustrate the full detail available in the images, we show blow-ups (Fig. 2) of the area around the N 11 (Henize 1956) complex. N 11 clearly has several compact features superimposed on a more extended fainter background. Such a phenomenon is very common to the large H II regions in the Magellanic Clouds. This smooth distributed emission is easier to see at 4.8 GHz where the low surface brightness is integrated over the larger beamwidth. The residual grating rings are also more obvious at that frequency for the same reason. In addition to N 11, the three faint blobs in the northeast of the 4.8 GHz image are the faint H II regions N 12, 13, and 14. The polarized source on the west side was labelled N 11L by Henize but is a well known supernova remnant and appears distinct from the thermal gas.

The integrated flux densities of all the components of N 11 (except N 11L) and the extended emission around them are 5.40 Jy at 4.8 GHz and 5.23 Jy at 8.64 GHz. The major uncertainty is in determining the outline of the source on the varying background of the LMC. Experimentation with various choices indicated an uncertainty of about 5 % or $\sim$0.3 Jy at both frequencies. The spectral index of N 11 from these measurements is -0.04, indicating its thermal nature. N 11L, on the other hand, has flux densities of 51 mJy at 4.8 GHz and 42 mJy at 8.64 GHz producing a spectral index is -0.32, clearly non-thermal.

3.2. *SMC*

The images of the SMC (Fig. 3) are certainly dominated by the H II region N 66 at about $00^{\rm h}59^{\rm m}15^{\rm s}$ and $-72°10'$ just north of the apparent and dynamical center of the SMC.

https://doi.org/10.1017/S1743921308028196 Published online by Cambridge University Press

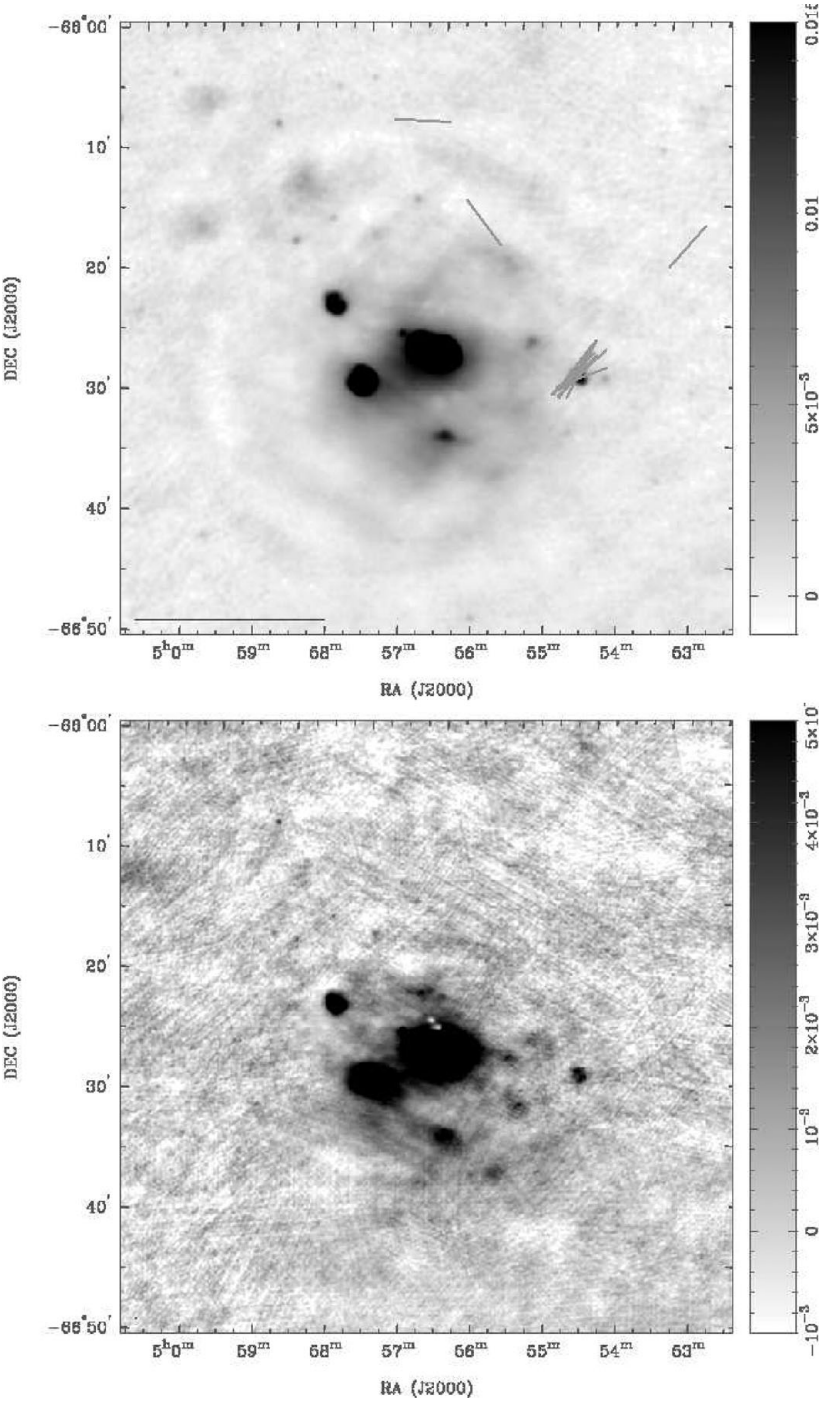

Figure 2. Total intensity image and polarization vectors of the large H II region complex N 11 in the northwest of the LMC at 4.8 GHz (top) and total intensity at 8.64 GHz (bottom). The line at the lower left of the top panel represents a polarized intensity of 5 mJy beam^{-1}. The significantly polarized source is the supernova remnant N 11L.

https://doi.org/10.1017/S1743921308028196 Published online by Cambridge University Press

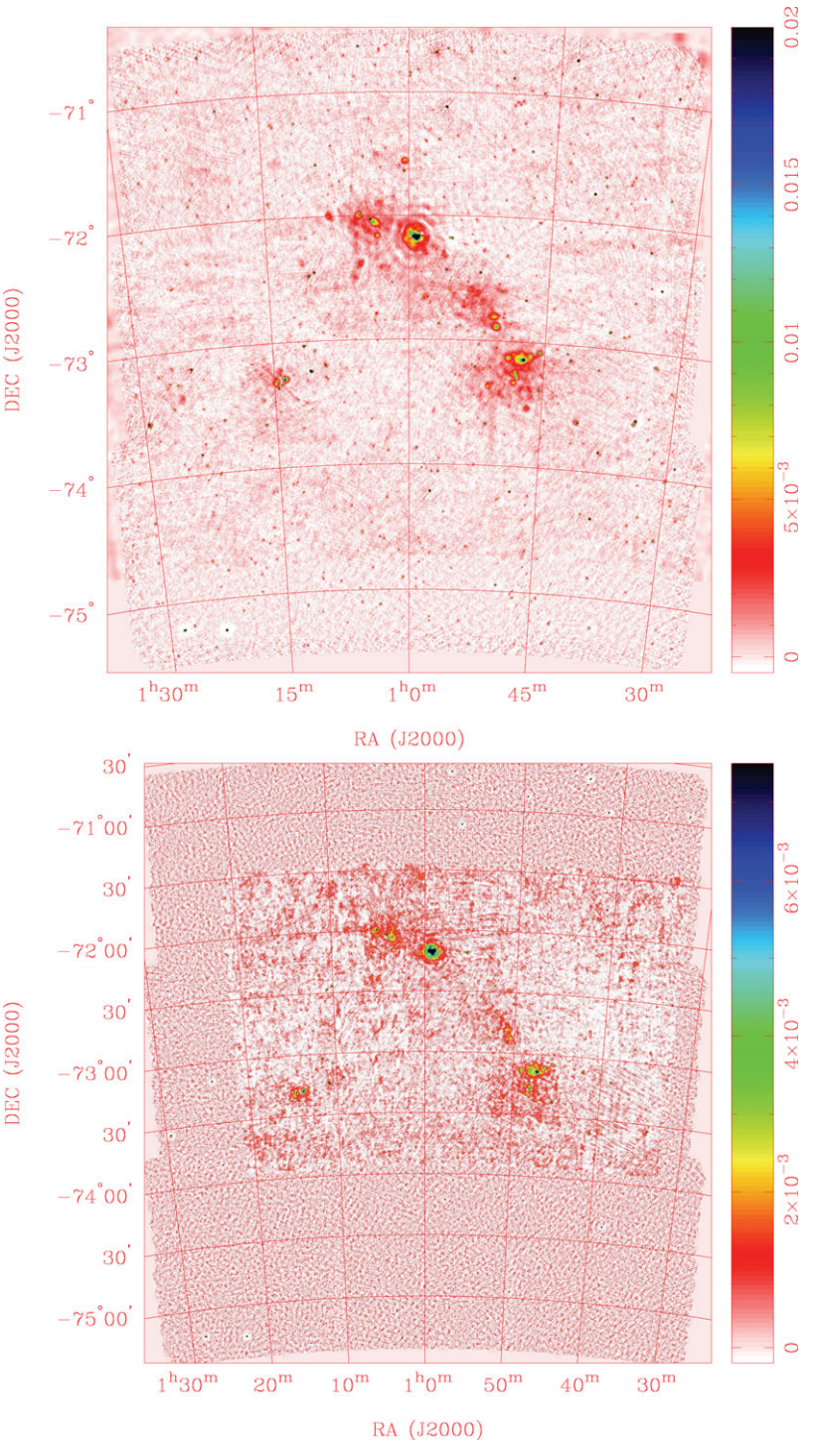

Figure 3. Total intensity image of the SMC at 4.8 GHz (top) and at 8.64 GHz (bottom).

https://doi.org/10.1017/S1743921308028196 Published online by Cambridge University Press

A number of other bright sources lie just east of there, including the very bright spot at $01^{\rm h}04^{\rm m}02^{\rm s}$ and $-72°01'55''$ which is the well known and brightest SNR in the SMC, E 0102.2−7219 (Seward & Mitchell 1981).

There is an indication of the bar off to the southwest ending near the bright feature N 19, a very confused area of H II regions and SNRs that still needs sorting out (Dickel *et al.* 2001) That area is near the major H I concentration in the galaxy (Stanimirović *et al.* 2004).

As with the LMC, most of the known SNRs and H II regions can be readily found in the expanded images. From the abrupt changes in the smoothness of the background, the reader can also see that the extent of the images from Parkes do not cover the full area of the *ATCA* ones. In particular, the 8.64-GHz image from Parkes is significantly smaller but still does cover most of the SMC sources. A few point sources appear around the edges where the data from Parkes are not available.

4. Data Availability

The calibrated UV data and the images, both total-intensity and polarimetric, are available in FITS format from the NCSA Astronomical Image Digital Library. The results can be downloaded from http://adil.ncsa.uiuc.edu/document/08.JD.01. The images include those from *ATCA* alone and merged ones from *ATCA* plus Parkes. We also provide filtered images so the 4.8- and 8.64-GHz images have the same *uv* range, though not identical coverage, of spacings in wavelengths to allow more careful spectral comparisons. The edited and calibrated *uv* data are also available in *MIRIAD* form from ADIL.

5. Acknowledgements

The Australia Telescope is funded by the Commonwealth of Australia as a National Facility managed by CSIRO. We have benefited from help and valuable discussions with many colleagues. They include Bob Sault, Lister Staveley-Smith, Uli Klein, Hélène Dickel, John Dickey, Robin Wark, Ray Plante, You-Hua Chu, Rosa Williams, Richard Rand, Gregory Taylor, Miroslav Filipović, and Brian Fields. Barry Parsons, Margaret House and Vicki Drazenovic helped to make the many visits to the Australia Telescope very enjoyable. Annie Hughes stimulated us to rethink the CLEANing procedures to produce more reliable images.

References

Bode, J. 1801, *General Description and Information of the Stars* (Berlin: privately published)

Cohen, R. S., Dame, T. M., Garay, G., Montani, J., Rubio, M., & Thaddeus, P. 1988, *ApJ*, 331, L95

Dickel, J. R., Williams, R. M., Carter, L. M., Milne, D. K., Petre, R., & Amy, S. 2001, *AJ*, 122, 849

Dickel, J. R., McIntyre, V. J., Gruendl, R. A., & Milne, D. K. 2005, *AJ*, 129, 790

Haynes, R. F., Klein, U., Wayte, S. R., *et al.* 1991, *A&A*, 252, 475.

Henize, K. 1956, *ApJS*, 2, 315

Högbom, J. A. 1973, *A&AS* 15, 417

Meixner, M. 2008, in Chary, R.-R., Tepliz, H., & Sheth, K. (eds.), *The Second Annual Spitzer Science Center Conference: Infrared Diagnostics of Galaxy Evolution, ASPSC*, 381, 115

Seward, F. & Mitchell, M. 1981, *ApJ*, 243, 736

Smith, R. C., Points, S., Chu, Y.-H., Winkler, P. F., Aguilera, C., & Leiton, R. 2005, *BAAS*, 37, 1403

Snowden, S. 1999, in Chu, Y.-H., Suntzeff, N., Hesser, J., & Bohlender, D. (eds), *New Views of the Magellanic Clouds, IAU Symposium 190, ASPSC*, 190, 32

Stanimirović, S., Staveley-Smith, L., & Jones, P. 2004, *ApJ*, 604, 176